

Neutron spin turners with a rotating magnetic field: first experiments

V I Bodnarchuk¹, W H Kraan², M T Rekveldt² and A Ioffe³

¹ Joint Institute for Nuclear Research, 141980 Dubna, Russia

² Interfaculty Reactor Institute, Delft University of Technology, Mekelweg 15, 2629JB, Delft, The Netherlands

³ Institut für Festkörperforschung, Forschungszentrum Jülich GmbH, Jülich Centre for Neutron Science at FRM II, Lichtenbergstr. 1, 85747 Garching, Germany

Received 12 October 2007, in final form 10 December 2007

Published 30 January 2008

Online at stacks.iop.org/MST/19/034012

Abstract

Spin turners are the key elements of a neutron spin-echo spectrometer with rotating magnetic fields. Here we describe the results of experiments with thin-film spin turners made of 25 μm amorphous ferromagnetic foils, whose in-plane magnetization is rotated by a weak external rotating field. The behaviour of the polarization vector of a 0.2 nm neutron beam is analysed in 3D after transmission through such a foil and, apart from a non-negligible depolarization, the results show that they are in good accordance with simulations. This observed depolarization is due to a domain structure with a net magnetization.

Keywords: neutron spin-echo spectroscopy, 3D polarization analysis, Larmor precession

Introduction

In a neutron resonance flipper [1] the neutron spin (seen in the rotating frame) rotates around an angle of π around the resonance magnetic field created by the superposition of two perpendicular magnetic fields: a constant field along the z -axis and a rotating one in the x - y plane. However, it is possible to achieve the same effect using a magnetic field rotating in the y - z plane of a thin spin turner (figure 1). If the neutron precession (Larmor) frequency $\omega L = \gamma \mathbf{B}$ defined by the magnetic field strength \mathbf{B} (γ is the gyromagnetic ratio for the neutron) is much higher than the frequency ω of the field rotation and the spin turner is thin enough, so that the vector \mathbf{B} is not rotated significantly during the neutron propagation across the spin turner, then, after the π -precession of the neutron spin around vector \mathbf{B} , it will again arrive in the y - z plane, i.e., effectively rotating with frequency 2ω around an instant position of the magnetic field vector.

Using such spin turners, it is possible to build a new type of spin-echo spectrometer, as schematically sketched in figure 2 [2]. As is explained there, as a result of propagation through the first SE-arm of length L_1 (spin turners 1 and 2, with \mathbf{B} rotating synchronously), the polarization rotates about the x -axis over an angle $\alpha(v) = \omega(L/v)$, irrespective of the direction of the magnetization at the arrival of a neutron at the first spin turner. Because of different propagation times for neutrons with different wavelengths, the polarization rotates by different

angles $\alpha(v)$, so that a non-monochromatic neutron beam will be fully depolarized. The second SE-arm (spin turners 3 and 4) is completely similar to the first arm; however, magnetic fields in these spin turners rotate in the opposite direction. This results in spin rotation over angles $-\alpha(v)$ and in the full restoration of the neutron beam polarization (both the magnitude and the direction) for any neutron velocity, i.e., for a non-monochromatic neutron beam. On the other hand, any changes of neutron velocities caused by inelastic scattering on a sample will lead to an uncompensated spin rotation that could be observed by polarization analysis. Thus, similar to the well-known generic NSE technique [4] the degree of the rotation of the polarization vector becomes a measure of inelastic scattering at the sample.

The aim of the present paper is to realize a rotating magnetic field of the required strength in a thin-foil spin turner by subjecting a soft-ferromagnetic foil to a weak rotating magnetic field.

Experimental details

As the working material for the spin turner we chose a thin foil of the metallic glassy alloy $\text{Fe}_{78}\text{B}_{13}\text{Si}_9$ of thickness 25 μm (fabricated by Goodfellow) that features a high-frequency susceptibility (300–500 kHz) and an extreme magnetic softness, so that an external magnetic field smaller than 50 mG is required to control the film magnetization.

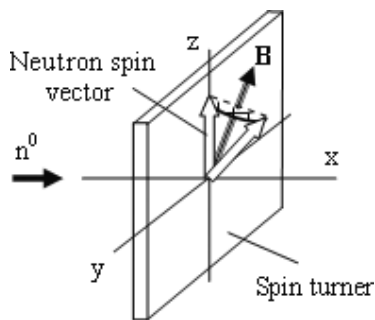


Figure 1. The principle of the spin turn device with a rotating magnetic field. The magnetic field vector **B** rotates in the plane *y-z* perpendicular to the neutron beam axis. The spin turner has such thickness that the neutron spin vector makes one-half of the full turn around the vector **B**, when propagating across the spin turner.

We put the foil into the field composition generated by the *y*-coil inside the *z*-coil, with fields $B_y = A_y \cos(\omega t)$ and $B_z = A_z \sin(\omega t)$ (see figure 3). When added, they produce the field rotating in the *y-z* plane at the circular frequency ω .

Currents in these coils are generated by two KEPCO amplifiers, controlled by the software of the spectrometer PANDA (TU Delft) [3]. The phase of KEPCO-*y* is delayed by 90° with respect to KEPCO-*z*. Data are collected in ‘dynamic mode’ in $N_{\text{chan}} = 100$ channels per revolution, coupled to the rotation of the field. When energizing *y*- and *z*-coils simultaneously, the currents are carefully adjusted to be equal and shifted by $\pi/2$ by an oscilloscope.

The response of a monochromatic ($\lambda = 0.2$ nm) polarized neutron beam is measured by 3D polarization analysis, after transmission through the coils system sketched in figure 4. In this instrument the polarization direction of the incoming beam can be adjusted to *x*, *y* or *z* when the transmitted

beam can independently be analysed along any of these axes. Each combination of settings (*i*, *j*) corresponds to the ‘depolarization matrix’ element D_{ij} given by $D_{ij} = 1 - (I_{ij}/I_s)$, where I_{ij} is the measured intensity and I_s the intensity at full depolarization of the beam.

Results

Characterization of field coils

To characterize the field coils we energized each coil separately and measured the full depolarization matrix of the transmitted beam without the sample. The amplitude of the current through the coils was set at 1.2 A, by observing the voltage over the 3.3Ω resistor in series with each coil. Measurements were taken by dividing the field period into $N = 100$ time channels at the low frequencies 500 Hz and 1 kHz. At any time the precession phase of the polarization vector during transmission through the coil system can be obtained from the elements of the depolarization matrix according to [3]

$$\begin{aligned} \varphi_y &= \arctan[(D_{xz} - D_{zx})/(D_{xx} + D_{zz})] && \text{(y-coil),} \\ \varphi_z &= \arctan[(D_{xy} - D_{yx})/(D_{xx} + D_{yy})] && \text{(z-coil).} \end{aligned} \tag{1}$$

To convert the time channel along the horizontal axis into the field, we applied the transformation

$$H_y = \sin\left(N\left(\frac{\pi}{50} - \varphi\right)\right), \tag{2}$$

where the ‘delay’ phase φ is found from the travel time $\tau = l_{\text{coils-det}}/v$ from the coils to the detector by

$$\varphi = 2\pi \frac{l_{\text{coil-det}}/v}{T}. \tag{3}$$

For 1 kHz (and $l_{\text{coil-det}} = 165$ cm; $v = 1980$ m s⁻¹; $T = 1000 \mu\text{s}$, the period of rotation) we obtained $\varphi = 5.6$ rad.

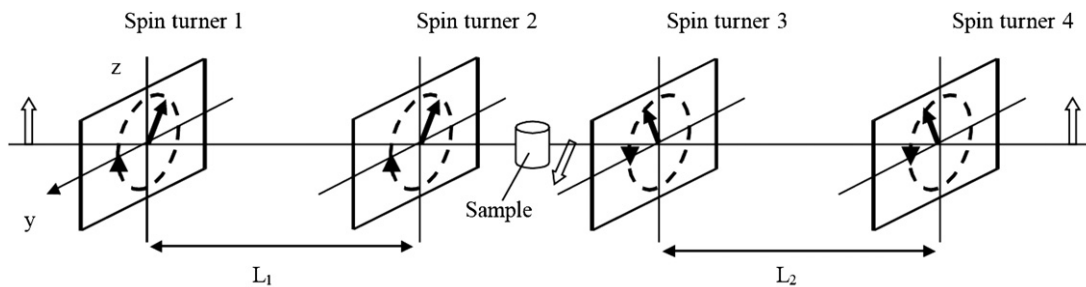


Figure 2. Layout of the NSE set-up with rotating magnetic fields [2].

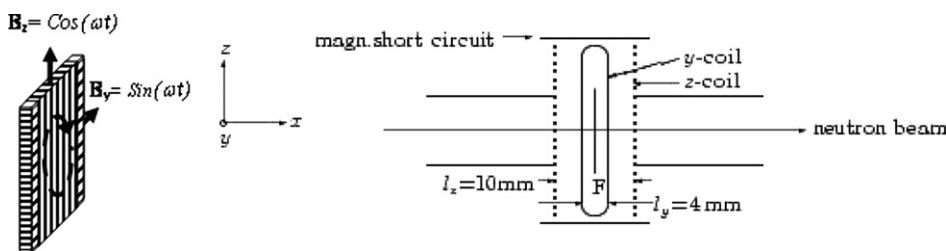


Figure 3. The coil configuration containing the foil F.

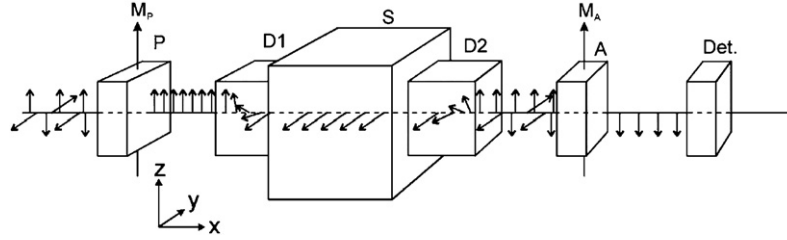


Figure 4. Schematic overview of the instrument PANDA at TU Delft. The arrows demonstrate the polarization vector evolution when the neutron beam passes through the PANDA 3D depolarization set-up. P—polarizer; M_p —magnetization vector of polarizer; D1—input coils oriented at the incoming spins along the necessary direction; S—‘zero-field’ chamber; D2—output coils mark the defined direction in 3D, on which spin projection will be measured; A—analyser; M_A —magnetization vector of the analyser; Det—single ^3He detector.

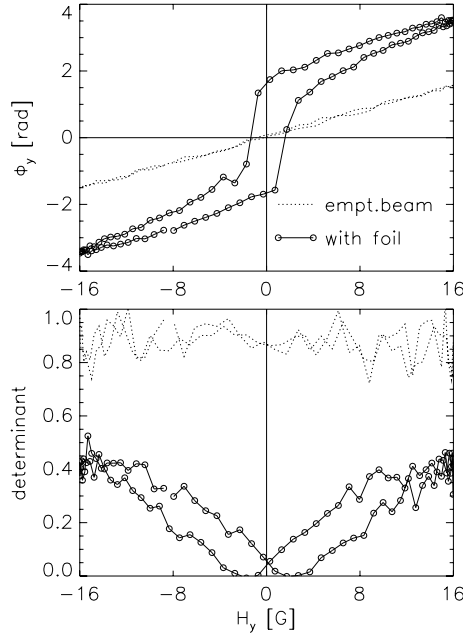


Figure 5. The rotation angle φ_y (equation (1)) of the polarization vector (top) and determinant (bottom) of the polarization matrix as a function of the magnetic field when energizing the y -coil only.

These results are presented as dotted lines in figure 5 (top). They show the precession phases φ_y as a function of the magnetic field at the current amplitude 1.2 A. Scales along the horizontal axes were calculated from the lines in the top of figure 5 according to

$$\varphi_y = c\lambda\mu_0 H_y l_y \quad (4)$$

($c = 4.63 \times 10^{14} \text{ T}^{-1} \text{ m}^{-2}$). Hence, for $\lambda = 0.2 \text{ nm}$ and $l_y = 4 \text{ mm}$ we obtain from the precession angle $\varphi_y = 1.5 \text{ rad}$ at the current amplitude 1.2 A (the right side of figure 5) that $B_y = \mu_0 H_y = 16 \text{ G}$. In a similar way we arrive from the precession angle $\varphi_z = 3.8 \text{ rad}$ and $l_z = 10 \text{ mm}$ at the current amplitude 1.2 A in the z -coil at the same value: $B_z = 16 \text{ G}$.

Characterization of magnetic foils

From the data with foil (solid lines) in figure 5 one reads from the right side that the foil produces a net rotation of 1.75 rad in the maximum field. For the foil of thickness $25 \mu\text{m}$, this allows us to estimate the maximum magnetic induction as $B = 0.76 \text{ T}$ (this is still not the full saturation

magnetization). Also, the determinant is still far from the determinant of the empty beam. An extrapolation suggests that the field should be at least 30 G to achieve saturation.

Foils in the rotating field

Initially, the maximal current amplitude was set at 1.2 A. Both with empty coils and with foils we could reach this amplitude up to the frequency of 20 kHz.

While the neutron beam propagates across the coil system, the polarization is subjected to the rotation $R(z)(\varepsilon)$ around z by the field of the outer coil before and after the inner coil, where $\varepsilon = c\lambda B_z(l_z - l_y)/2$ with $B_z = B_z^{\max} \cos(\omega t)$. We transform the argument ωt into the time channel n by means of $\omega t = 2\pi(n/N)$ where N is the total number of time channels. To account for the delay $\tau = l_{\text{foil-det}}/v$ between the foil and the detector, ωt is diminished by φ given by equation (2). Hence, the rotation ε in the z -field before and after the inner coil is given by

$$\begin{aligned} \varepsilon &= \left(c\lambda |B| \frac{l_z - l_y}{2} \right) \cos\left(2\pi \frac{n}{N} T - \varphi \right) \\ &\equiv \varepsilon' \cos\left(2\pi \frac{n}{N} T - \varphi \right). \end{aligned} \quad (5)$$

When entering the inner coil (y), the polarization vector is subjected to the rotating magnetic field denoted \vec{B} . We describe the rotation in this field in the coordinate system, where the vector \mathbf{B} remains pointing along the z direction by the (3×3) matrix $R(z)(\Phi)$, and

$$\Phi = c|\vec{B}|\lambda l_y. \quad (6)$$

Transformed into the laboratory system, this matrix becomes

$$R^{(x)}(\theta)R^{(z)}(\Phi)R^{(x)}(-\theta) \quad (7)$$

where the angle $\theta = \omega t$ between the positive z -axis and the rotating field, in analogy with the phase of B_z , is written as follows:

$$\theta = 2\pi \frac{n}{N} T - \varphi. \quad (8)$$

Here we neglect the field component along the rotation axis $x B_x = \omega/\gamma$. Hence, the complete transformation undergone by the polarization vector reads

$$\begin{aligned} R(\varepsilon, \Phi, n, \varphi) &= R^{(z)}(\varepsilon)R^{(x)}(\theta(n, \varphi)) \\ &\times R^{(z)}(\Phi)R^{(x)}(-\theta(n, \varphi))R^{(z)}(\varepsilon), \end{aligned} \quad (9)$$

where ε , Φ and $\theta(n, \varphi)$ are given by equations (5)–(7). They contain ε' , Φ and φ as parameters. Equation (5) for the lengths

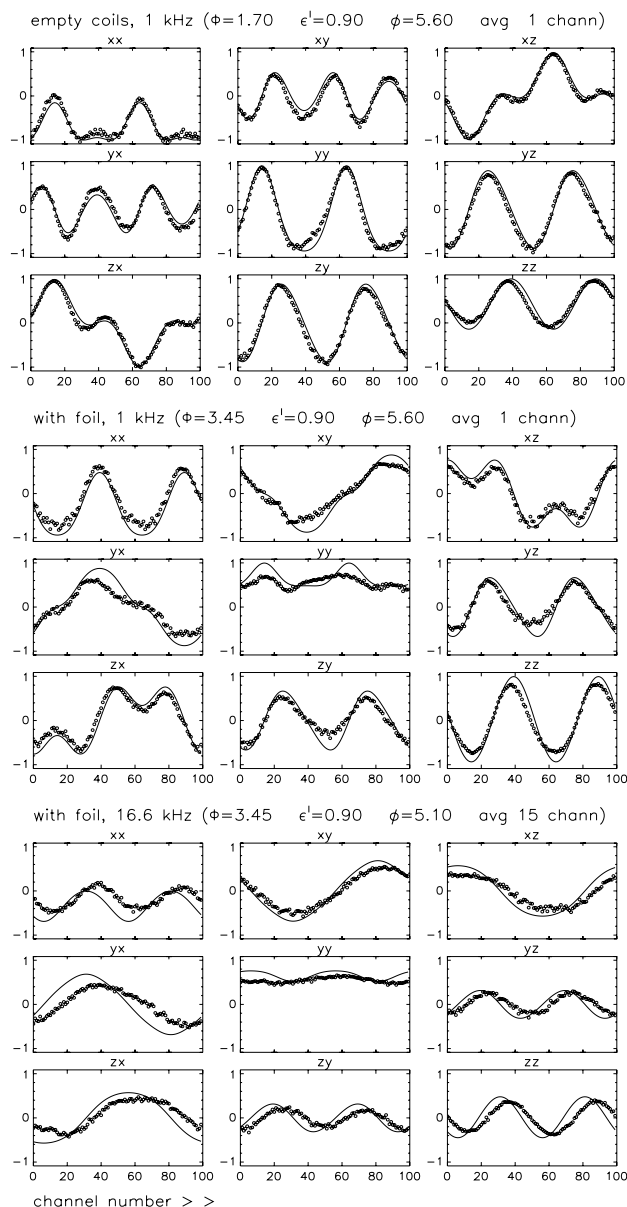


Figure 6. Elements of the depolarization matrix with rotating magnetic fields, measured (circles) and calculated according to equation (9) (lines) as a function of the time channel in one cycle of the field: (a) empty coil system, 1 kHz; (b) with the foil, 1 kHz, (c) with the foil, 16.6 kHz. It is seen at 16.6 kHz that the measured matrix elements 'lag behind' the calculated elements by about seven channels.

l_y and l_z given above, combined with $|B| = 16$ G, gives $\varepsilon' = 0.9$. Equation (6) in the case of an empty coil gives $\Phi = 1.7$, and when the foil is mounted $\Phi = 3.45$. Above we found for 1 kHz: $\varphi = 5.6$ rad.

Figure 6(a) contains the depolarization matrix elements for the empty coil system at 1 kHz; figure 6(b) gives the same, with the foil in the coil system. The lines refer to the results calculated according to equation (9) with properly chosen ε' , Φ and φ as parameters. The simulation gives a rather consistent description of the observed matrices, especially

at low frequencies. This is seen from comparing the data points at 1 kHz (circles) with the full lines (simulations). At higher frequencies the phenomena become smeared over time channels, as to be expected from the wavelength spread of PANDA.

For the simulation at frequencies above 10 kHz, equation (2) gives values for the parameter φ more than ten times 2π within a precision of 5%. Reduced between 0 and 2π , this parameter gets an uncertainty corresponding to the half field period. To obtain a more precise value we carried out simulations for the empty beam measurements, choosing φ in such a way that the simulations coincide with measurements. These values of φ were used to simulate measurements with the foil; figure 6(c) (see parameters below) shows the result for 16.6 kHz. Measured matrix elements appear to be shifted by about 7 channels ($\sim 4 \mu\text{s}$) towards the calculated data. This means that the magnetization in the foil 'lags behind' the imposed rotating field. At 20 kHz this effect amounts to $6 \mu\text{s}$. Simultaneously, we observe that the determinant decreases with increasing frequency. Both phenomena indicate the presence of a domain structure, which becomes increasingly difficult to eliminate at higher frequencies, so a much stronger field is required to achieve the foil's saturation at higher frequencies.

Conclusions

We have shown that the intended field configuration is reasonably realized and the behaviour of the observed polarization vector corresponds to the calculations. The increasing depolarization and the fact that the magnetization lags behind the rotating field at 16 kHz suggests that the proposed concept of a ferromagnetic foil with rotating magnetization for a spin turner has a limited range (5–10 kHz) of frequencies. From the point of view of applications of such foils, for purposes of rotating magnetic field neutron spin-echo spectroscopy it means a limited range in the spin-echo time; in SESANS a limited maximum spin-echo length. Perhaps the reason for the high depolarization is the domain structure in the studied amorphous ferromagnetic foil. Indeed, the present alloy needs a much stronger field (>30 G) to be fully magnetized; so for our practical purposes another alloy may be required.

Acknowledgment

The project has been supported by the European Commission under the 6th Framework Programme through the Key Action: Strengthening the European Research Area, Research Infrastructures (contract no: HII3-CT-2003-505925).

References

- [1] Gähler R and Golub R 1988 Neutron resonance spin echo, bootstrap method for increasing the effective magnetic field *J. Physique* **49** 1195–202
- [2] Ioffe A 2003 Wide angle high-resolution spectroscopy at pulsed neutron sources *Physica B* **335** 169–73

- [3] Rekveldt M Th 1973 Study of ferromagnetic bulk domains by neutron depolarization in three dimensions *Z. Phys.* **259** 391–410
Rekveldt M Th 1971 Neutron depolarisation as a method to determine the magnetization, the mean domain size and the mean square components of the inner magnetization of ferromagnets *J. Physique Coll.* **32** C1 579–81
- [4] Mezei F 1972 Neutron spin echo: a new concept in polarized thermal neutron techniques *Z. Phys.* **255** 146